

2. Computational method

We performed the first-principles calculations by the Atomistix Toolkit (ATK) package, which is based on the combination of density functional theory (DFT) and non-equilibrium Green's function technique [17]. The mesh cutoff energy is chosen as 150 Ry, and the k -point mesh is $1 \times 1 \times 100$ [18]. The Perdew-Burke-Ernzerhof formulation of the generalized gradient approximation (GGA) have been used as the exchange-correlation function, and the double-zeta polarized basis set is employed in the calculations. The size of the scattering region cell of bare ZGNR ($a \times b \times c$) is set to be $10.00 \times 20.00 \times 27.01 \text{ \AA}^3$, and the size of the electrode cell is $10.00 \times 20.00 \times 4.92 \text{ \AA}^3$. In our models, as the carbon chain length increases, the size of the b -axis direction of the central scattering area increases from 20.00 to 28.00 \AA . In order to prevent the interaction with adjacent images, the vacuum spaces of supercell are set to be more than 10 \AA . All the atomic positions of the structure have been optimized, until all residual forces on each atom are smaller than 0.02 eV/ \AA . The edges of ZGNRs are terminated with hydrogen (H) atoms to remove the dangling bonds. The two-probe device is divided into three parts: the left semi-infinite ZGNR electrode, the central scattering region and the right semi-infinite ZGNR electrode (as shown in Fig. 1). The carbon chains are placed at the center of the scattering region edge, and contain N carbon atoms. In this study we choose $N=1$ to 6 configurations to study, which are referred to C1–C6.

3. Results and discussions

In the C1–C6 models, the C1, C3 and C5 are odd-numbered chains configurations, and the C2, C4 and C6 belong to even-numbered chains structures. Through the structural optimization, we found that all the length of C–H bond remain to be 1.08 \AA which are unchanged corresponding to that of bare ZGNR as shown in Fig. 2. The adjacent C–C bonds of even-numbered chains structures obviously differ in length, up to 0.19 \AA , so their carbon chains' bonding pattern can be qualitatively assigned to alternat-ing single and triple bonds showing obvious polyene properties.

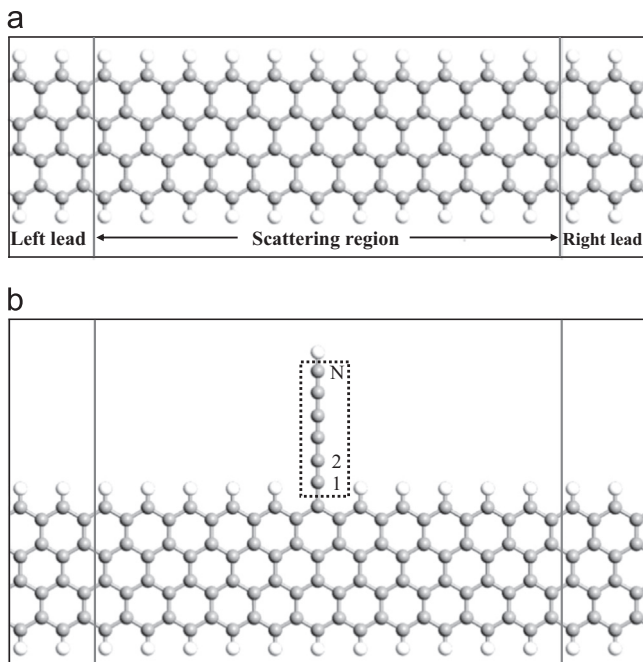


Fig. 1. Schematic illustration of (a) bare model; (b) CN model (N is the number of carbon atoms in the chain, from 1 to 6).

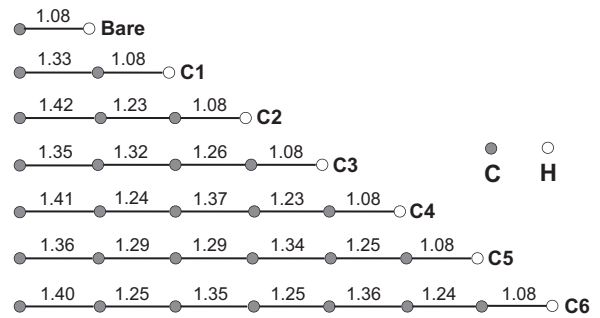


Fig. 2. Bond length of bare and C1–C6 configurations, in unit of \AA . The left end of the carbon chain is connected to the ZGNR as shown in Fig. 1. For clarity, only the carbon chains are drawn, the ZGNRs are not shown here.

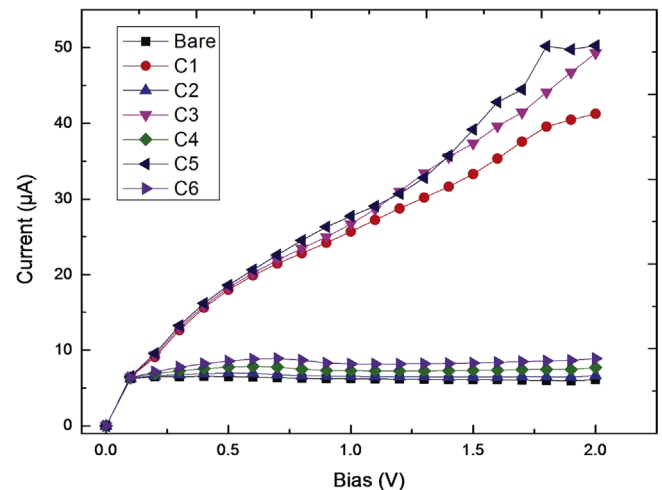


Fig. 3. (Color online) The current-voltage curves of bare and C1–C6 model in bias range from -2.0 to 2.0 V.

However, for odd-numbered chains, all the C–C bond lengths are similar, and these configurations are π -conjugated structures which present polyolefin properties [15,14].

The current-voltage (I - V) characteristics of all models are presented in Fig. 3. When the bias is below 0.1 V, all the curves are the same. However, as the bias increases, the shape of the I - V curves of even-numbered configurations are same as that of bare ZGNR. Only slight increase of the current with the increase of the chain length is observed. On the contrary, the currents of odd-numbered cases are larger than those of even models, and they increase when the bias increases, showing ohmic characteristics. So, we could conclude that the electron transport properties strongly depend on the chains' odd-even structure [19,20].

In order to investigate the physical origin of the odd-even characteristics in the I - V curves of these models, we first calculate their corresponding transmission spectra and the molecular projected self-consistent Hamiltonian (MPSH) under bias $V_b=1.0$ V, as shown in Fig. 4. It can be found that, around the Fermi energy, odd-numbered configurations have three transmission peaks, however the even-numbered ones have an obvious suppression, which is similar to the bare ZGNR [Fig. 4(a) and (b)]. The transmittance spectra of the even-numbered models decrease distinctly in the range from -0.5 to 0.5 eV. To better compare their transmission spectra, we take C3 and C4 models as examples to study the electronic structure for odd- and even-numbered cases respectively. In Fig. 4(c), the highest occupied molecular orbital (HOMO), HOMO-1 and HOMO-2 locate below the Fermi level in the integral area, indicated by the shaded area. The lowest unoccupied molecular orbital (LUMO) lies on the right edge of the

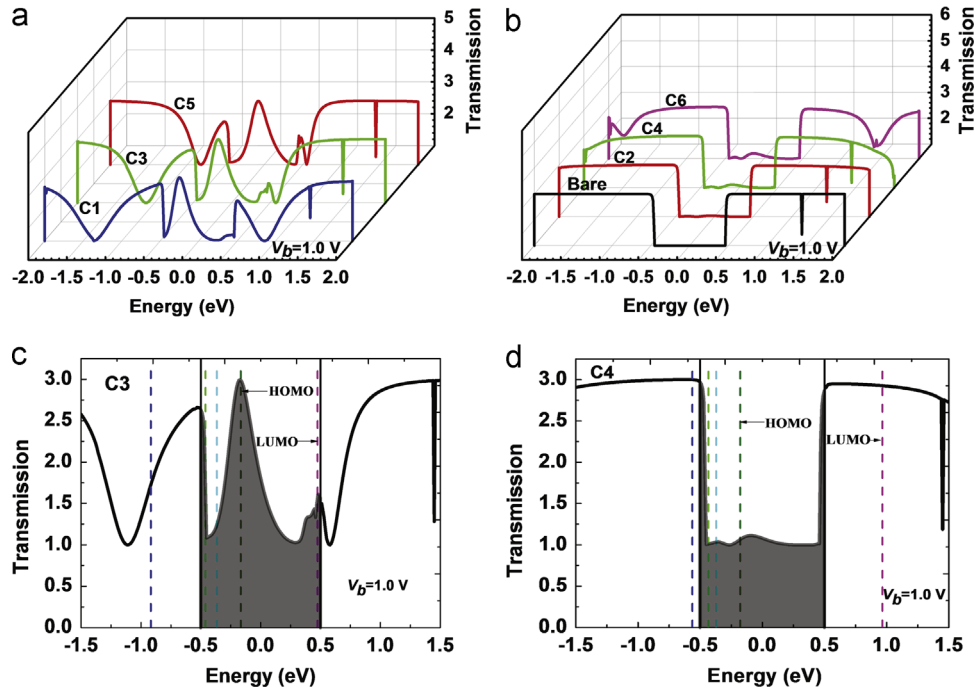


Fig. 4. (Color online) The transmission spectra of (a) odd-numbered chains junctions; (b) bare and even-numbered chains junctions; (c) C3 model; (d) C4 model under bias $V_b = 1.0$ V. In (c) and (d), the region between the solid lines is the bias window, the shaded area indicates the integral area and the vertical dash lines represent the corresponding molecular orbitals. Zero energy is the Fermi level.

integral area. Among them, HOMO and HOMO-1 are the nearest orbitals to the Fermi level, so the electron transport is mainly dominated by HOMO and HOMO-1 [21]. In the bias window, there appears a big transmission peak contributed by HOMO, so the integral area becomes larger, and the current of C3 model increases obviously. In Fig. 4(d), we can find that the positions of HOMO, HOMO-1, HOMO-2 nearly do not change. However the LUMO lies outside of the bias window, which means its contribution is suppressed [21]. In the bias window there exist two small transmission peaks contributed by HOMO-1 and HOMO respectively, so the current of C4 model increases slightly.

In Fig. 4, we could see that there is an obvious decrease in the I - V curves of the bare and even-numbered models, but none in that of odd-numbered chains junctions. Li et al. [22] have reported that the symmetry of the GNR plays an important role in the electron transport. They discover that the conductance of symmetric ZGNRs is smaller than that of asymmetric ones because a conductance gap emerges around the Fermi level. This difference is attributed to different subbands coupling. In our research we find the same mechanism. Fig. 5(a) shows the unit cell structure of the bare ZGNR. We calculated its band structure (see Fig. 5(b)). From the middle inset, it is easy to see that there are two partially flat bands near the Fermi level without bias [23]. The π and π^* subbands are derived from these two edge states, they are respectively corresponding bonding state and the anti-bonding states [22,24,25]. If we apply a positive bias (V_+)/negative one (V_-) on the electrode, the band structure will shift upward/downward, as shown in the left and right panels of Fig. 5(c). As a result, there appears an energy window (the shadow region) due to the Fermi level shifts. In Fig. 5(c), we give out the wave functions of π and π^* subbands. It is easy to see that the π subband has odd parity, nevertheless, the π^* subband has even parity under σ mirror operation. As shown in Fig. 5(b), in the shadow region there are only π subband in the V_+ region while only π^* subband in the V_- region. Because the π and π^* subbands have opposite σ parity, an electron belongs to π subband can not hop to a π^* state so that these subbands can not contribute to the transmission and an obvious suppression

emerges as shown in Fig. 5(e). The transmission of the bare nanoribbon is not equal to zero, which could be attributed to the coupling of the two edge sides. When we reduce the width of bare ZGNR to from 4 to 3 as shown in the inset of Fig. 5(d), the bare ZGNR becomes a asymmetric structure. Li et al. [22] have reported that the energy state of asymmetric ZGNRs have no σ parity. We calculated the transmission spectrum of this asymmetric bare ZGNR, and it is clear that the transmission is nearly a straight line under bias $V_b = 1.0$ V, as shown in Fig. 5(d). Compared with this, our bare model has an obvious suppression as shown in Fig. 5(e). Therefore, if the system has σ parity, the transmission will decrease, and the current will become small. Our bare and even-numbered carbon chain models are corresponding to this. On the contrary, if the σ parity of the system is destroyed, the π and π^* subbands can couple with each other, and a suppression will not appear in the transmission, so the current will be larger. Our odd-numbered configurations are corresponding to this, and its transmission tends to revert to the situation of the asymmetric structure as shown in Fig. 5(f).

In order to further investigate the state of our models, we regarded the scattering region of our model as a periodic configuration, then calculated its bandstructures. Fig. 6(a) presents the wave functions of the two subbands nearest to the Fermi level. Most of the wave functions are delocalized, but in the odd-numbered configurations (C1, C3 and C5), one of the two wave functions concentrates in the center region. Moreover, it is obviously that all the wave functions of the two subbands of bare and even-numbered junctions have σ parity in the horizontal direction of transport, while those of the odd-numbered junctions not. Next we attach the electrode to the left and right sides of the scattering region and investigate the influence of electrodes on it. We calculated the MPSH eigenstates of the molecular orbitals HOMO-1 and HOMO which are the nearest levels to the Fermi level for all our models. The MPSH states are calculated by projecting the Hamiltonian of the whole two-probe system onto the scattering region and diagonalizing the new Hamiltonian. Then we could treat the scattering region as an isolated molecule, which

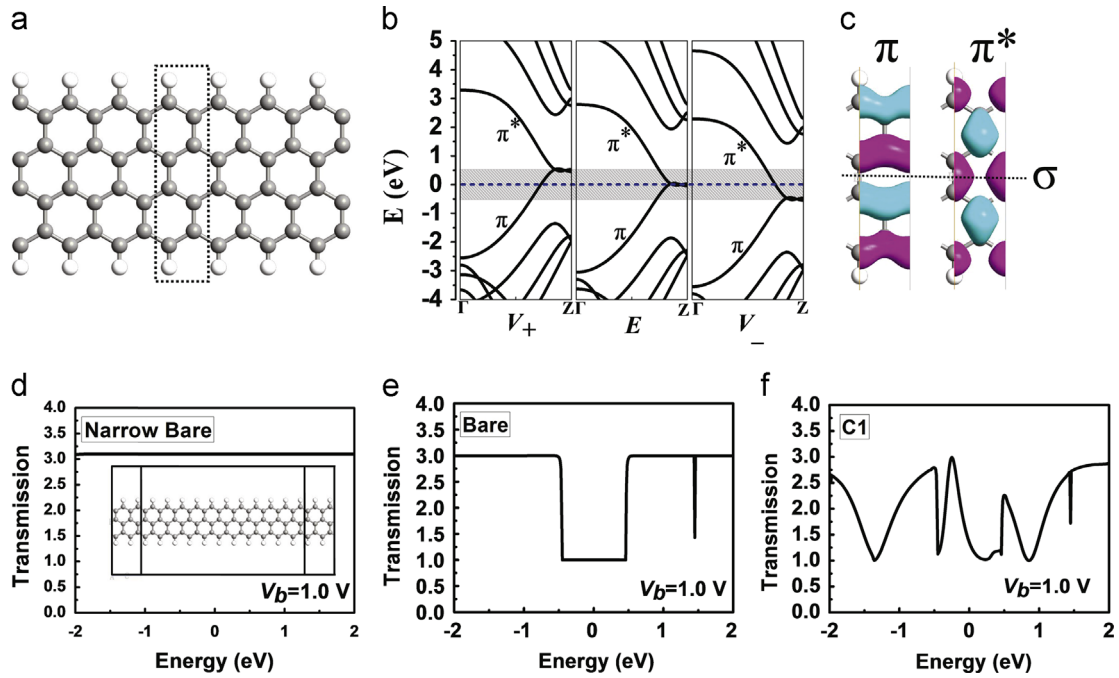


Fig. 5. (Color online) (a) The schematic illustration of the selected ZGNR, the dashed box indicates the primitive cell. (b) Band structure around the Fermi level. The left is under positive bias, the middle is without bias and the right is under negative bias. (c) Isosurface plots of the Γ -point wave functions of π and π^* subbands. (d) The transmission coefficients of narrow bare model which has a smaller width of three carbon atoms, and its structure schematic illustration is shown in the inset. (e) The transmission coefficients of bare model. (f) The transmission coefficients of C1 model.

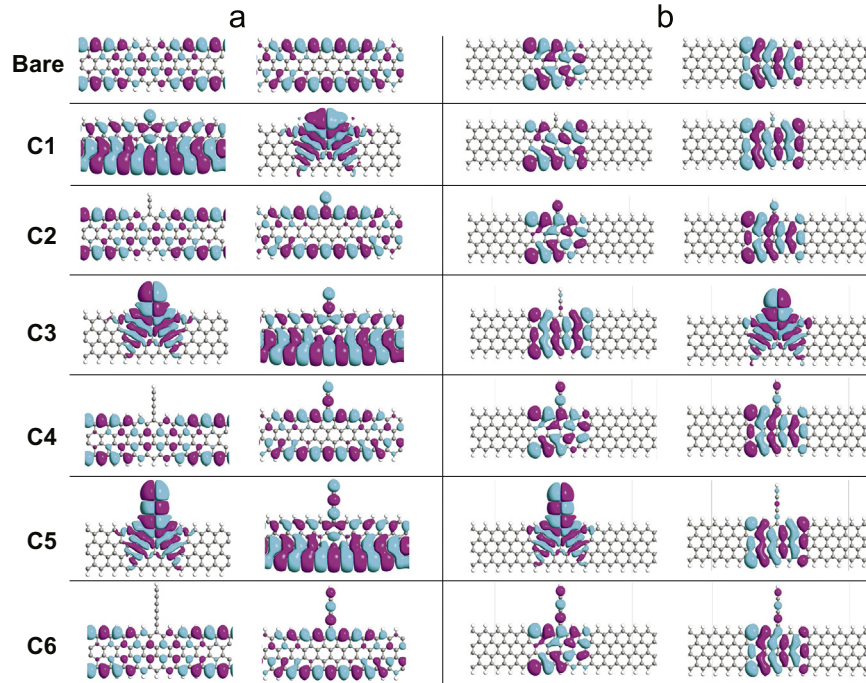


Fig. 6. (Color online) (a) Isosurface plots of the wave functions of two nearest subbands to the Fermi level for the scattering region of bare and C1–C6 model. The k -points mesh used in the calculation is $1 \times 1 \times 15$. (b) The MPSH of the HOMO-1 and HOMO molecular orbitals for bare and C1–C6 model.

has taken into account effect of the electrodes. Related MPSH states are the eigenstates of the molecular system placed in a two-probe environment [26]. In Fig. 6(b), again, the MPSH of the bare and even-numbered junctions have σ parity in the horizontal direction of transport while the odd-numbered junctions do not have. Consequently, the even-numbered and odd-numbered junctions have completely different electron transport properties.

In the condition of the anti-ferromagnetic (AFM) state, all the MPSH eigenstates have no σ parity in the horizontal direction of transport and result in large current, in agreement with the mechanism we discussed above. However, it is different from that of spin-unpolarized case for even-numbered configurations, where σ parity exists. This is a very interesting phenomenon, and we hope to do a systematic research in future studies.

4. Conclusion

In summary, using first-principles calculations, we have studied the transport properties of the ZGNR with upright standing linear carbon chains. The carbon chains' bonding pattern in even-numbered chains (C2, C4 and C6) junctions shows obvious poly-yne properties while the pattern in odd-numbered chains (C1, C3 and C5) structures presents polyolefin properties. The configurations with upright standing linear carbon chains show significant odd-even dependence of transport properties, i.e., the bare and even-numbered models show similar I - V characteristics and only small leakage current is found, while the odd-numbered models show metallic, and their currents are much larger than those of even models. Further studies show that, the odd-even parity of carbon chains would influence the σ parity of ZGNR's electronic states, and then results in the odd-even disparity of transport behaviors. Different from previous studies, the carbon chain in our system is not in (or along) the main transport direction of the electronic transmission. As related structures have been realized in experiment, our results might be quite useful for the development of carbon-based nanoelectronic devices.

Acknowledgments

This work is supported by the National Natural Science Foundation of China (NSFC51032002, NSFC11374162, and NSFC11247033), the Scientific Research Foundation of Nanjing University of Posts and Telecommunications (NY214010), and the Fundamental Research Funds for the Central Universities (NS2014073).

References

- [1] P. Avouris, Z. Chen, V. Perebeinos, *Nat. Nanotechnol.* 2 (10) (2007) 605–615.
- [2] A.K. Geim, K.S. Novoselov, *Nat. Mater.* 6 (3) (2007) 183–191.
- [3] I. Deretzis, G. Fiori, G. Iannaccone, A. La Magna, *Phys. Rev. B* 81 (8) (2010) 085427.
- [4] Z. Zhang, J. Zhang, G. Kwong, J. Li, Z. Fan, X. Deng, G. Tang, *Sci. Rep.* 3 (2575).
- [5] M.Y. Han, B. Özyilmaz, Y. Zhang, P. Kim, *Phys. Rev. Lett.* 98 (20) (2007) 206805.
- [6] V. Barone, O. Hod, G.E. Scuseria, *Nano Lett.* 6 (12) (2006) 2748–2754.
- [7] Ç.Ö. Girit, J.C. Meyer, R. Erni, M.D. Rossell, C. Kisielowski, L. Yang, C.-H. Park, M. Crommie, M.L. Cohen, S.G. Louie, et al., *Science* 323 (5922) (2009) 1705–1708.
- [8] E.-j. Kan, Z. Li, J. Yang, J. Hou, *J. Am. Chem. Soc.* 130 (13) (2008) 4224–4225.
- [9] Z. Zanolli, G. Onida, J.-C. Charlier, *ACS Nano* 4 (9) (2010) 5174–5180.
- [10] L. Ravagnan, F. Siviero, C. Lenardi, P. Piseri, E. Barborini, P. Milani, C. Casari, A.L. Bassi, C. Bottani, *Phys. Rev. Lett.* 89 (28) (2002) 285506.
- [11] L. Ravagnan, P. Piseri, M. Bruzzi, S. Miglio, G. Bongiorno, A. Baserga, C. Casari, A.L. Bassi, C. Lenardi, Y. Yamaguchi, et al., *Phys. Rev. Lett.* 98 (21) (2007) 216103.
- [12] J.C. Meyer, C.O. Girit, M. Crommie, A. Zettl, *Nature* 454 (7202) (2008) 319–322.
- [13] A. Chuvilin, J.C. Meyer, G. Algara-Siller, U. Kaiser, *New J. Phys.* 11 (8) (2009) 083019.
- [14] C. Jin, H. Lan, L. Peng, K. Suenaga, S. Iijima, *Phys. Rev. Lett.* 102 (2009) 205501, <http://dx.doi.org/10.1103/PhysRevLett.102.205501>.
- [15] M. Qiu, K.M. Liew, *EPL (Europhys. Lett.)* 101 (6) (2013) 68005.
- [16] L. Shen, M. Zeng, S.-W. Yang, C. Zhang, X. Wang, Y. Feng, *J. Am. Chem. Soc.* 132 (33) (2010) 11481–11486.
- [17] M. Brandbyge, J.-L. Mozos, P. Ordejón, J. Taylor, K. Stokbro, *Phys. Rev. B* 65 (16) (2002) 165401.
- [18] H. Monkhorst, J. Pack, *Phys. Rev. B* 13 (1976) 5188.
- [19] K.H. Khoo, J. Neaton, Y.W. Son, M.L. Cohen, S.G. Louie, *Nano Lett.* 8 (9) (2008) 2900–2905.
- [20] N. Lang, P. Avouris, *Phys. Rev. Lett.* 81 (16) (1998) 3515.
- [21] A. Li-Ping, L. Chun-Mei, L. Nian-Hua, *Commun. Theor. Phys.* 57 (6) (2012) 1087.
- [22] Z. Li, H. Qian, J. Wu, B.-L. Gu, W. Duan, *Phys. Rev. Lett.* 100 (20) (2008) 206802.
- [23] M. Fujita, K. Wakabayashi, K. Nakada, K. Kusakabe, *J. Phys. Soc. Japan* 65 (7) (1996) 1920–1923.
- [24] K. Wakabayashi, M. Sigrist, *Phys. Rev. Lett.* 84 (15) (2000) 3390.
- [25] T. Martins, R. Miwa, A.J. da Silva, A. Fazio, *Phys. Rev. Lett.* 98 (19) (2007) 196803.
- [26] S. Sen, S. Chakrabarti, *J. Phys. Chem. C* 112 (5) (2008) 1685–1693.